sciendo

DOI 10.2478/ama-2022-0021

acta mechanica et automatica, vol.16 no.3 (2022)

DESIGN AND ANALYSIS OF A NOVEL CONCEPT-BASED UNMANNED AERIAL VEHICLE WITH GROUND TRAVERSING CAPABILITY

Ramanuj KUMAR*, Surjeet S. GOUR*, Anish PANDEY*, Shrestha KUMAR*, Abhijeet MOHAN*, Pratik SHASHWAT*, Ashok K. SAHOO*

*School of Mechanical Engineering, Kalinga Institute of Industrial Technology Deemed to be University, An Institute of Eminence, Patia, Campus-8, Bhubaneswar, 751024, Odisha, India

ramanujfme@kiit.ac.in, surjeetgour59@gmail.com, anish06353@gmail.com, 1602403@kiit.ac.in, 1602389@kiit.ac.in,1602351@kiit.ac.in, asahoofme@kiit.ac.in

received 26 November 2021, revised 16 February 2022, accepted 1 March 2022

Abstract: Unmanned aerial vehicle (UAV) is a typical aircraft that is operated remotely by a human operator or autonomously by an on-board microcontroller. The UAV typically carries offensive ordnance, target designators, sensors or electronic transmitters designed for one or more applications. Such application can be in the field of defence surveillance, border patrol, search, bomb disposals, logistics and so forth. These UAVs are also being used in some other areas, such as medical purposes including for medicine delivery, rescue operations, agricultural applications and so on. However, these UAVs can only fly in the sky, and they cannot travel on the ground for other applications. Therefore, in this paper, we design and present the novel concept-based UAV, which can also travel on the ground and rough terrain as an unmanned ground vehicle (UGV). This means that according to our requirement, we can use this as a quadcopter and caterpillar wheel–based UGV using a single remote control unit. Further, the current study also briefly discusses the two-dimensional (2D) and three-dimensional (3D) SolidWorks models of the novel concept-based combined vehicle (UAV + UGV), together with a physical model of a combined vehicle (UAV + UGV) and its various components. Moreover, the kinematic analysis of a combined vehicle (UAV + UGV) has been studied, and the motion controlling kinematic equations have been derived. Then, the real-time aerial and ground motions and orientations and control-based experimental results of a combined vehicle (UAV + UGV) are presented to demonstrate the robustness and effectiveness of the proposed vehicle.

Key words: unmanned aerial vehicle, unmanned ground vehicle, rough terrain, quadcopter, caterpillar wheel, kinematic analysis

1. INTRODUCTION

1.1. Background and literature review

Unmanned aerial vehicles (UAVs) come under low-cost, light-weight and low airspeed aircraft, which are generally used to obtain aerial photographs [1] and in other remote sensing data collections. However, it is not easy to take aerial images in dense forest conditions with existing UAVs [2] . Therefore, in this condition, we can go for an unmanned ground vehicle (UGV) to capture the photographs. Further, we need a common vehicle, which can work as a UAV and UGV simultaneously according to our requirements and environmental conditions. UAV problems [3] can be divided into various categories such as navigation, motion planning, trajectory tracking, surveillance and so on. Moreover, these problems can be mathematically represented through the Newton–Euler method or Lagrangian formula, and both methods are applied for an underactuated complex UAV system. The purpose of trajectory tracking is to control the motion of a quadcopter in a predefined path by calculating the rotor velocities of a quadcopter. UAVs are also known as drones, and they have a simple mechanical chassis and are mainly lifted and propelled by four independent blades or rotors. In addition, these UAVs come in different sizes, shapes and number of rotors. Glida et al. [4] presented the dynamic analysis of a quadcopter. They optimised the various controlling parameters such as roll, pitch and yaw angles by implementing a cuckoo search optimisation algorithm. Labbadi and Cherkaoui [5] used the Euler–Newton formula to design the dynamic model for a quadcopter. They tried to solve the external disturbance problem using the proportional integral derivative (PID) sliding mode control. However, in that investigation, only computer simulation results were displayed, and real-time experimental results were not obtained. Hassani et al. [6] used Newtonian formalism and designed a robust adaptive non-linear controller to solve the path-tracking problem of a quadcopter under disturbed environment conditions.

Most researchers [4, 5, 6, 7] have tried to solve the trajectory tracking problems under disturbed conditions. However, they have only shown the computer simulation results in their work, and have not reported the real-time experiment results of a quadcopter. A particle swarm optimisation (PSO)-tuned adaptive neuro-fuzzy inference system (ANFIS) controller is implemented by Selma et al. [7] to achieve a robust trajectory tracking scheme for a three-degree freedom quadcopter in a disturbed environment condition. An extensive review article on motion planning of quadcopters or drones and their various control techniques was reported by Elijah et al. [8] , and although these authors discussed the physical results associated with the experimental deployment of a quadcopter, they were not elaborately reported in that work. Moreover, Heidari and Saska [9] briefly discussed the different types of quadcopters such as fixed-wing and multi-rotor and their

advantages and disadvantages in various applications with a comparative analysis. The research by Abdalla and Al-Baradie [10] integrated the PSO algorithm with the PID controller to design a steer control scheme for a quadcopter. The cognitive architecture-based decision-making control method for UAVs was designed by Pinto et al. [11].

Route planning with optimum path selection is also an important problem in UAV motion. Many researchers have also addressed this problem, and some related works [12, 13, 14, 15, 16] are cited here. Route planning for a quadcopter or UAV is to search the optimal flight path from the source point to a destination to reduce the time and energy [12]. Therefore, Xu et al. [12] implemented a gravitational search algorithm to address this issue. The MATLAB graphical user interface module was used to show the different 2D and 3D flight motion results. Another similar type of work was found in an article by Zhang and Duan [13] , in which the authors applied a differential evolution algorithm for the global route planning of a UAV in a 3D environment. Further, previous studies applied some more optimisation algorithms such as the genetic algorithm (GA) [14] , ant colony optimisation (ACO) [15] , water drops optimisation algorithm [16] and hybrid GA [17] to search feasible optimal routes for UAVs. However, they have not focused on designing a UAV and its real-time experimental results. Silva et al. [17] used the flight-gear simulator to show the fly motion results of a UVA under different wind speeds and directions. Comparative performance analysis of different multi-objective evolutionary algorithms as a path planner of UAV has been studied by Besada-Portas et al. [18]). Cui and Wang [19] implemented the reinforcement learning algorithm to design local and global path planners for a UAV among static and moving obstacles. Yao and Zhao [20] suggested the model predictive control algorithm to search optimal or sub-optimal collision-free trajectories for a UAV in the midst of dynamic obstacle conditions. However, Besada-Portas et al. [18]; Cui and Wang [19]; and Yao and Zhao [20] have shown the software-based computer simulation results of UAVs in their studies. Heidari and Saska [9] developed a heuristic approach–based open-loop control system to select optimal values of the dynamic control parameters such as thrust force and torque of a quadcopter for trajectory optimisation.

After summarising the above-cited scientific literature, we find that most of the work has been based on either trajectory tracking control or path planning of a UAV or quadcopter. Moreover, many authors have only presented the software-based simulation results in their studies, and they have not focused on any new concept-based quadcopter designing. Therefore, we have tried to design and fabricate the novel concept-based UAV in this work, which can also travel on the ground and rough terrain, as a UGV.

1.2. Important contribution

This paper's contributions are summarised as follows: First, a new concept-based combined vehicle (UAV + UGV) is designed and fabricated, which can fly as a quadcopter or UAV, and it can also travel on the ground, rough terrain and rough narrow paths as a UGV or a wheeled robot. Next, the various kinematic equations are explained briefly and embedded in the microcontroller. Then, the flying and ground motion and orientation of the UAV and caterpillar wheel–based UGV are controlled during navigation through a single control unit or remote controller. Further, the SolidWorks model of a combined vehicle (UAV + UGV) and its various connected parts is briefly discussed with different 2D and 3D pictorial representations. Finally, the other equipped electronic hardware components of a combined vehicle (UAV + UGV) and its real-time flying and ground motions and orientation results are presented to demonstrate the robustness and effectiveness of the designed vehicle.

1.3. Paper organisation

The rest of the paper is organised as follows: Section 2 reveals the kinematic equations for the UAV and its attached caterpillar wheel–based UGV arrangement, which are applied to control the flying and ground motion and orientation of the whole vehicle. The various 2D and 3D SolidWorks models of a combined vehicle (UAV + UGV) are presented in Section 3. Section 4 briefly discusses the various electronic components of a combined vehicle (UAV + UGV) and shows the real-time experimental results. Finally, Section 5 provides the salient points of the current investigation, together with the conclusions reached.

2. KINEMATIC STUDY OF THE UAV AND ITS ATTACHED CATERPILLAR WHEEL–BASED UGV

This section reveals the kinematic equations for the UAV and its attached caterpillar wheel–based UGV, which are used to control the flying and ground motion and orientation of a combined vehicle (UAV + UGV). Fig. 1 shows the pictorial representation of various kinematic and dynamic indices of only UAV in the 3D workspace.

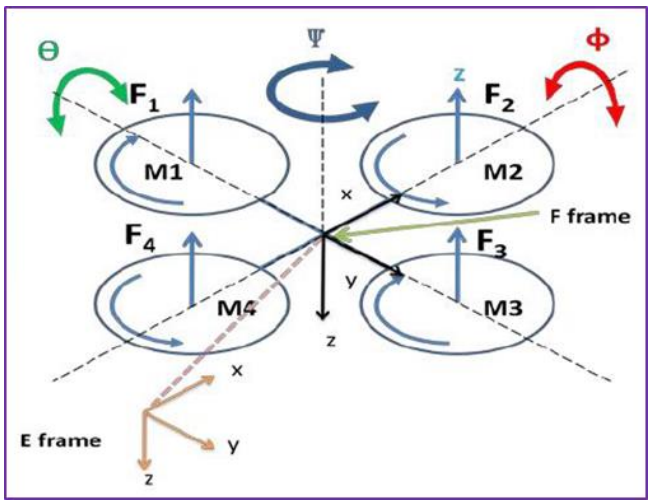

Fig. 1. Pictorial representation of various kinematic and dynamic indices of only UAV in the 3D workspace. UAV, unmanned aerial vehicle

Lightweight glass fibre is used to construct the frame of the UAV because the structural rigidity of this glass fibre is high. The centre part of the frame carries various electronic components such as flight controller, motor driver, receiver, battery, Arduino microcontroller and so on. The frame also has four spider arms protruding from it, which accommodate brushless DC motors, and the motors provide sufficient rotational motions to the rotors. These rotors are fixed to the tip of motors and produce adequate thrust to lift off a combined vehicle. The arms also consist of the

electronic speed controller (ESC) for controlling the rotational speed of the motors, and the ESC controls the directions of the UAV. This UAV performs six motions in total (three translations and three rotations) by using its attached four rotors, and it consists of multiple input and output control systems. In Fig. 1, $A_E = [X_E, Y_E, Z_E]^T$ defines the absolute linear position vector of the UAV and $\dot{A}_E = \left[\dot{X}_E, \dot{Y}_E, \dot{Z}_E\right]^T$ represents the linear velocity vector with respect to the E reference frame in the 3D workspace. The $\alpha = [\theta, \phi, \Psi]^T$ is the angular displacement or attitude vector with respect to the E reference frame, where ϕ, θ and Ψ reveal the Euler angles of roll, pitch and yaw, respectively. A combined vector $q = [A_E, \alpha]^T$ represents the linear and angular position vectors of the UAV. Similarly, $A_F = [x_F, y_F, z_F]^T$ defines the absolute linear position vector of the UAV and $\dot{A}_F = [\dot{x}_F, \dot{y}_F, \dot{z}_F]^T$ represents the linear translation velocity vector with respect to the F body frame in the 3D workspace. And $\beta = [\dot{m}, \dot{n}, \dot{o}]^T$ defines the angular velocity vector with respect to the F body frame. The kinematic study of the UAV reveals the relationship between the reference frame and the body frame [5] . The rotation and translation kinematic equations can be described as follows:

$$R_R = \begin{bmatrix} c(\theta)c(\Psi) & s(\phi)s(\theta)c(\Psi) - c(\phi)s(\Psi) & c(\phi)s(\theta)c(\Psi) + s(\phi)s(\Psi) \\ c(\theta)s(\Psi) & s(\phi)s(\theta)s(\Psi) + c(\phi)c(\Psi) & c(\phi)s(\theta)c(\Psi) - s(\phi)c(\Psi) \\ -s(\theta) & s(\phi)c(\theta) & c(\phi)c(\theta) \end{bmatrix} \tag{1}$$

$$\begin{bmatrix} \dot{X}_E \\ \dot{Y}_E \\ \dot{Z}_E \end{bmatrix} = R_R \cdot \dot{A}_F = \begin{bmatrix} c(\theta)c(\Psi) & s(\phi)s(\theta)c(\Psi) - c(\phi)s(\Psi) & c(\phi)s(\theta)c(\Psi) + s(\phi)s(\Psi) \\ c(\theta)s(\Psi) & s(\phi)s(\theta)s(\Psi) + c(\phi)c(\Psi) & c(\phi)s(\theta)c(\Psi) - s(\phi)c(\Psi) \\ -s(\theta) & s(\phi)c(\theta) & c(\phi)c(\theta) \end{bmatrix} \cdot \begin{bmatrix} \dot{x}_F \\ \dot{y}_F \\ \dot{z}_F \end{bmatrix} \tag{2}$$

$$\dot{X}_E = \dot{x}_F \cdot \left(c(\theta)c(\Psi)\right) + \dot{y}_F \cdot \left(s(\phi)s(\theta)c(\Psi) - c(\phi)s(\Psi)\right) + \dot{z}_F \cdot (c(\phi)s(\theta)c(\Psi) + s(\phi)s(\Psi)) \tag{3}$$

$$\dot{Y}_E = \dot{x}_F \cdot (c(\theta)s(\Psi)) + \dot{y}_F \cdot (s(\phi)s(\theta)s(\Psi) + c(\phi)c(\Psi)) + \dot{z}_F \cdot (c(\phi)s(\theta)c(\Psi) - s(\phi)c(\Psi)) \tag{4}$$

$$\dot{Z}_E = \dot{x}_F \cdot (-s(\theta)) + \dot{y}_F \cdot (s(\phi)c(\theta)) + \dot{z}_F \cdot (c(\phi)c(\theta)) \tag{5}$$

where R_R describes the rotational matrix for the UAV from the F body frame to the E reference frame and c and s denote the cosine and sine trigonometry terms, respectively. The angular transformation matrix R_T from the F body frame to the E reference frame can be formulated as:

$$R_T = \begin{bmatrix} 1 & s(\phi)t(\theta) & c(\phi)t(\theta) \\ 0 & c(\phi) & -s(\phi) \\ 0 & \frac{s(\phi)}{c(\theta)} & \frac{c(\phi)}{c(\theta)} \end{bmatrix} \tag{6}$$

where t symbolises the tangent trigonometry term. After calculating the linear velocities of the UAV, we calculate the values of angular velocities from the F body frame to the E reference frame as:

$$\begin{bmatrix} \dot{\theta} \\ \dot{\phi} \\ \dot{\Psi} \end{bmatrix} = R_T \cdot \beta = \begin{bmatrix} 1 & s(\phi)t(\theta) & c(\phi)t(\theta) \\ 0 & c(\phi) & -s(\phi) \\ 0 & \frac{s(\phi)}{c(\theta)} & \frac{c(\phi)}{c(\theta)} \end{bmatrix} \cdot \begin{bmatrix} \dot{m} \\ \dot{n} \\ \dot{o} \end{bmatrix} \tag{7}$$

$$\dot{\theta} = \dot{m} + \dot{n} \cdot \left(s(\phi)t(\theta)\right) + \dot{o} \cdot \left(c(\phi)t(\theta)\right) \tag{8}$$

$$\dot{\phi} = \dot{n} \cdot \left(c(\phi)\right) - \dot{o} \cdot \left(s(\phi)\right) \tag{9}$$

$$\dot{\Psi} = \dot{n} \cdot \left(\frac{s(\phi)}{c(\theta)}\right) + \dot{o} \cdot \left(\frac{c(\phi)}{c(\theta)}\right) \tag{10}$$

For the dynamic equations of motion for the UAV, we consider the Newton–Euler formula [5, 6].

The caterpillar wheel–based UGV is made up of lightweight glass fibre panels and joined with the base of the UAV's frame using nut and bolt. The two holes on each side of the fibre panels are punched to connect the four DC motors, and these motors are attached with the caterpillar driving wheels, which carry the mechanical frame. The two caterpillar driving wheels set, connected on the left side of a combined vehicle (UAV + UGV), are controlled as a left-wheel driving system. Similarly, another two caterpillar driving wheels set, attached on the right side of a combined vehicle, are completely run on the ground as a right-wheel driving system. U_L denotes the left-wheel driving system, and U_R represents the right-wheel driving system in the kinematic equations. Fig. 2 illustrates the graphical representation of various kinematic and dynamic indices of the caterpillar wheel–based UGV system in the 2D workspace.

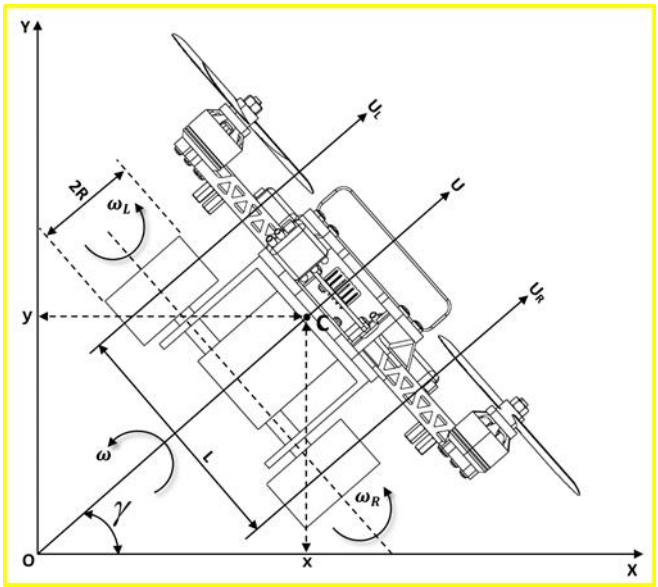

Fig. 2. Graphical representation of various kinematic and dynamic indices of caterpillar wheel–based UGV system in the 2D workspace (UGV, unmanned ground vehicle)

The axes (x, y) are the current location of the UGV system from the origin O point in the global frame $\{O, X, Y\}$. In Fig. 2, γ indicates the steering control angle of the UGV with respect to an axis (O, X), L is the track width between the left and right driving systems, R is the radius of the wheel and C is the centre of mass of the UGV. The following kinematic equations control the velocities and steering angle of the UGV:

$$U = \frac{R}{2} \cdot (\omega_R + \omega_L) = \frac{U_R + U_L}{2} \quad (11)$$

$$\omega = \dot{\gamma} = \frac{R}{L} \cdot (\omega_R - \omega_L) = \frac{U_R - U_L}{L} \quad (12)$$

where U and ω symbolise the centre (mean) linear velocity and centre angular velocity of the UGV, respectively. These U and ω control the motion and orientation of the UGV in the C/C++ microcontroller programming, respectively. Next, ω_R and $\omega_L$represent the angular velocities of the right-wheel driving system and left-wheel driving system, respectively.

Further, the following equations express the velocity (linear and angular) with respect to time:

$$\frac{dx}{dt} = \dot{x}(t) = U \cdot \cos\gamma = \frac{R}{2}(\omega_R + \omega_L) \cdot \cos\gamma \quad (13)$$

$$\frac{dy}{dt} = \dot{y}(t) = U \cdot \sin\gamma = \frac{R}{2} \cdot (\omega_R + \omega_L) \cdot \sin\gamma \quad (14)$$

$$\frac{d\theta}{dt} = \dot{\gamma}(t) = \omega = \frac{R}{L} \cdot (\omega_R - \omega_L) \quad (15)$$

Next, the following conditions are used for the linear and angular motion controls of the UGV:

1. If $(U_R = U_R)$, then the UGV travels straight.
2. If $(U_R > U_R)$, then the UGV turns left.
3. If $(U_R < U_R)$, then the UGV turns right.

3. BRIEF DESCRIPTION OF THE VARIOUS COMPONENTS OF THE UAV AND ITS ATTACHED CATERPILLAR WHEEL–BASED UGV

This section provides a brief description of various components of a combined vehicle (UAV + UGV). We have used SolidWorks software to design the prototype model, and we have presented the different 2D and 3D views of a combined vehicle (UAV + UGV). Figs. 3–8 illustrate the various 2D and 3D views of a combined vehicle (UAV + UGV). Tab. 1 (ESC, electronic speed controller; UAV, unmanned aerial vehicle; UGV, unmanned ground vehicle.) summarises the defined part numbers and names of the various components of a combined vehicle (UAV + UGV). A brief description of some figures and the connections of various components has been provided below.

Tab. 1. Part numbers and names of the various components of a combined vehicle (UAV + UGV)

Part Number	Part Name
1	Rotors or blades
2	Brushless motors for rotors
3	Electronic system box
4	Right wheel driving system
5	Left wheel driving system
6	UGV's frame
7	Spider arms
8	DC motors for UGV's wheels
9	Shafts of right side DC motors
10	Shafts of Left Side DC Motors
11	UAV's frame
12	Bolt to connect arms
13	Nut
14	ESC

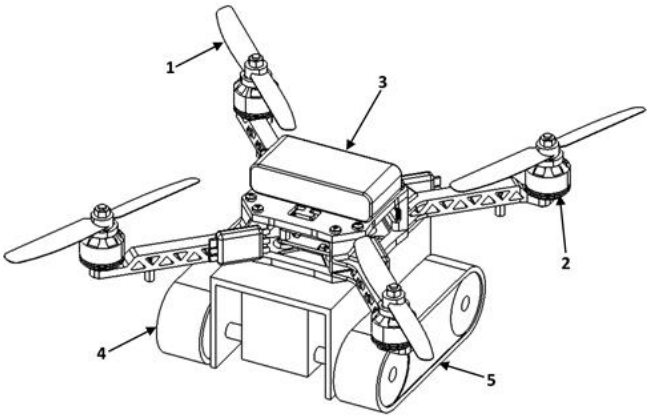

Fig. 3. Isometric view of a combined vehicle (UAV + UGV), (UAV, unmanned aerial vehicle; UGV, unmanned ground vehicle)

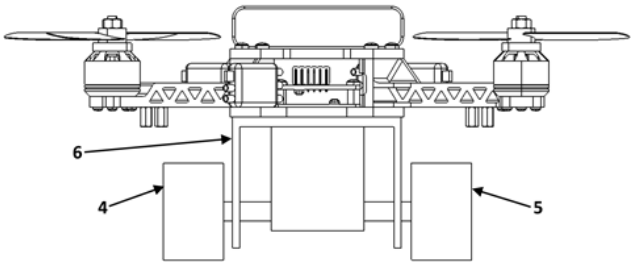

Fig. 4. Front view of a combined vehicle (UAV + UGV), (UAV, unmanned aerial vehicle; UGV, unmanned ground vehicle)

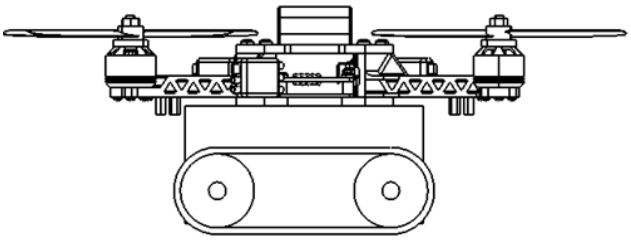

Fig. 5. Side view of a combined vehicle (UAV + UGV), (UAV, unmanned aerial vehicle; UGV, unmanned ground vehicle)

As illustrated in Fig. 3, the proposed vehicle (UAV + UGV) includes rotors or blades (1), brushless motors for rotors (2), an electronic system box (3), right wheel driving system (4), left wheel driving system (5), a UGV's frame (6) and a UAV's frame (11). The ground traversing device or UGV facilitates the whole vehicle (UAV + UGV) to traverse the ground or any terrain. In a vehicle (UAV + UGV), the electronic system box (3) is used to control the flying and ground motions and orientation of the aerial driving mechanism and ground traversing mechanism. The electronic system box (3) includes one transceiver configured to communicate between the remote control and vehicle and transfers the data, e.g. video or image data and commands, enabling the electronic system box (3) to control the aerial driving and the ground traversing mechanism. This electronic system box (3) is configured to control the aerial driving mechanism and the ground traversing mechanism independently. In a combined vehicle (UAV + UGV), the electronic system box (3) may include one or more sensors configured to measure one or more attributes pertaining to, by way of example but not limited to, location, environment and properties of the ground surface. For example, a combined vehicle (UAV + UGV) may include ground penetrating radar

(GPR) sensors that may sense one or more properties of the ground surface, such as but not limited to the type of rock, soil and ice; availability of freshwater; pavements; and structures. With the help of the GPR sensors, the UAV can detect improvised explosive devices (IED) and landmines, which is advantageous in the field of defence. Moreover, it can be useful in research areas where the surface changes in materialistic property need to be detected.

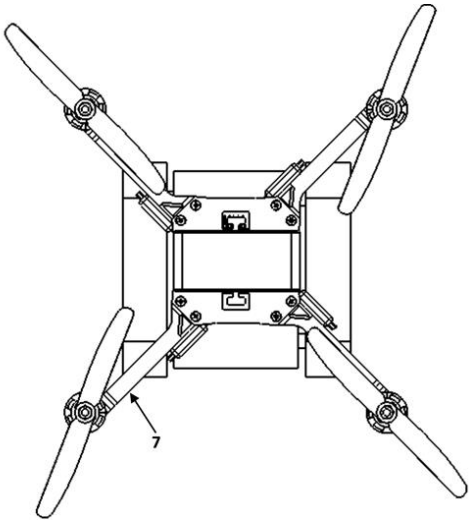

Fig. 6. Top view of a combined vehicle (UAV + UGV), (UAV, unmanned aerial vehicle; UGV, unmanned ground vehicle)

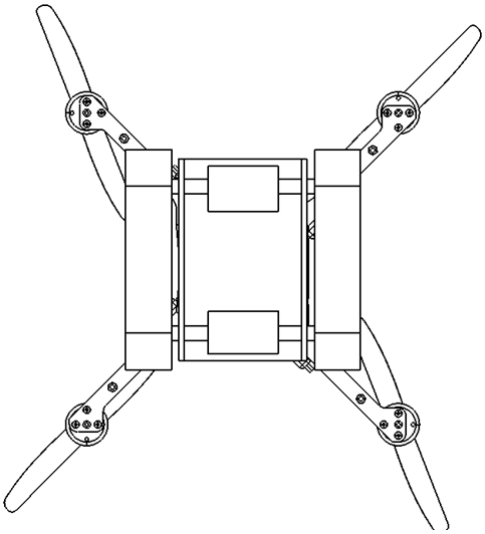

Fig. 7. Bottom view of a combined vehicle (UAV + UGV), (UAV, unmanned aerial vehicle; UGV, unmanned ground vehicle)

The electronic system box (3) includes a calibration unit and a compass unit. The calibration unit may allow, for example, the calibration of a vehicle (UAV + UGV) regarding a predefined plane in a coordinate system, e.g. to determine the roll and pitch angle of a vehicle (UAV + UGV) with respect to the gravity vector (e.g. from planet Earth). Thus, an orientation of a vehicle (UAV + UGV) in a coordinate system may be determined. The orientation of a vehicle (UAV + UGV) may be calibrated using the calibration unit before a vehicle (UAV + UGV) is operated in-flight modus. However, any other suitable function for navigation of a vehicle (UAV + UGV), e.g. for determining a position, a flight velocity, a flight direction and so on, may be implemented in the electronic system box (3). In a vehicle (UAV + UGV), the UAV's frame (11) includes a camera to capture an image of the surroundings and to provide the captured image to the microcontroller of an electronic system box (3). This electronic system box (3) is configured to process the captured images and determine one or more attributes pertaining to the object. For example, the electronic system box (3) identifies the position of objects in the image. The electronic system box (3) consists of a transmitter that may be configured to transmit information such as, but not limited to, information about the captured image to a server or the remote location.

Fig. 8 depicts an exploded view of a combined vehicle (UAV + UGV), which indicates all the important components of a vehicle. The UAV's driving assembly includes rotors or blades (1), spider arms (7) and brushless motors (2) for aerial movement. In an aspect, the UAV's driving assembly consists of four brushless motors (2), and motors (2) are attached with the spider arm (7). In a vehicle (UAV + UGV), the UAV's frame also includes a driving circuit ESC (14) that is attached to the brushless motors (2). The driving circuit may also be operatively connected to the electronic system box (3). The electronic system box (3) provides an input signal to the driving circuits to drive the brushless motors (2). In a UAV's driving assembly, the rotors or blades (1) are configured to rotate in at least two anticlockwise and clockwise directions. The rotation of rotors or blades (1) provides an upward lift to the UAV and facilitates a vehicle (UAV + UGV) to move in the air. In a vehicle (UAV + UGV), the ground traversing device or UGV includes the UGV's frame (6), caterpillar wheel–based right-wheel driving system (4), left-wheel driving system (5) and DC motors (8). The ground traversing device is attached to the lower portion of the UAV's frame (11). The configuration of the ground traversing device with the vehicle enables the vehicle to traverse on the surface, i.e. provides the ground traversing capability. In a vehicle (UAV + UGV), the ground traversing device includes a control unit to control the rotation of the DC motors (8). The control unit is implemented as a hardware component in an electronic system box (3). In a different embodiment, the control unit is implemented as a computer program product, which includes a computer-readable storage medium employing a set of instructions. The ground traversing device also consists of the DC motors (8) configured to rotate selectively in clockwise and anticlockwise directions. The motor driver of the ground traversing device controls the direction of the rotation of the DC motors (8) and the amount of the rotation of the DC motors (8).

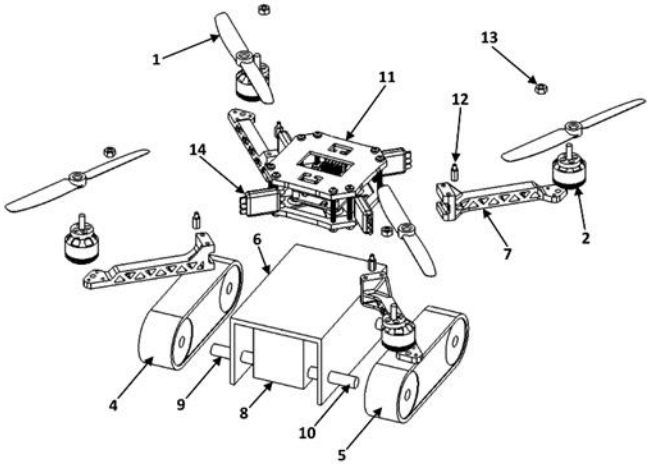

Fig. 8. Exploded view of all the components of a combined vehicle (UAV + UGV), (UAV, unmanned aerial vehicle; UGV, unmanned ground vehicle)

The ground traversing device also includes a caterpillar wheel–based right-wheel driving system (4) and a left-wheel driving system (5) operatively coupled to the shafts of the right-side DC motors (9) and the left-side DC motors (10), respectively, and configured to rotate in the clockwise and anticlockwise directions. The coupling of DC motors (8) enables the caterpillar wheel–based right wheel driving system (4) and left wheel driving system (5) to rotate in the direction of the rotation. Particularly, the rotation of the DC motors (8) in a clockwise direction facilitates the rotation of the caterpillar wheels in a clockwise direction, and the rotation of the DC motors (8) in an anticlockwise direction provides the rotation of the caterpillar wheels in an anticlockwise direction. In an embodiment, the ground traversing device or UGV system is attached to the existing vehicle to provide the ground traversing capability. The electronic box system (3) provides the input to the driving circuits to drive the DC motors (8). As illustrated in Fig. 8, the UGV's frame (6) of the ground traversing device is attached to the lower portion of a UAV's frame (11). This UGV's frame (6) is attached to UAV's frame (11) by bolt (12) and nut (13). The UGV's frame (6) of the ground traversing device is attached to the aerial driving assembly, at its one side that is opposite to another side of the UGV's frame (6), at which the wheel and DC motors (8) are attached for the ground traversing mechanism.

4. EXPERIMENTAL STUDY

This section briefly discusses the various electronic components of a combined vehicle (UAV + UGV). It also presents the experimental results to demonstrate the effectiveness of the developed vehicle in real-time applications. In addition, we describe the working principle of various electronic components that are used in a vehicle. Fig. 9 A–E illustrates snapshots of the different views (isometric, top, bottom, front and side) of the physical model of a combined vehicle (UAV + UGV). Moreover, this figure shows the various electronic components of a vehicle. The chassis and spider arms of a combined vehicle (UAV + UGV) are made up of lightweight glass fibre. A combined vehicle's length, width and height are 60 cm, 60 cm and 16 cm, respectively. The length of each spider arm is 49 cm. Similarly, the track width and wheelbase distance of the UGV's caterpillar driving wheels are 26 cm and 21 cm, respectively. The attached electronic components of a vehicle and their specifications are given in Tab. 2 (ESC, electronic speed controller; UAV, unmanned aerial vehicle; UGV, unmanned ground vehicle). The vehicle's ground and aerial motions are controlled with the help of these electronic components.

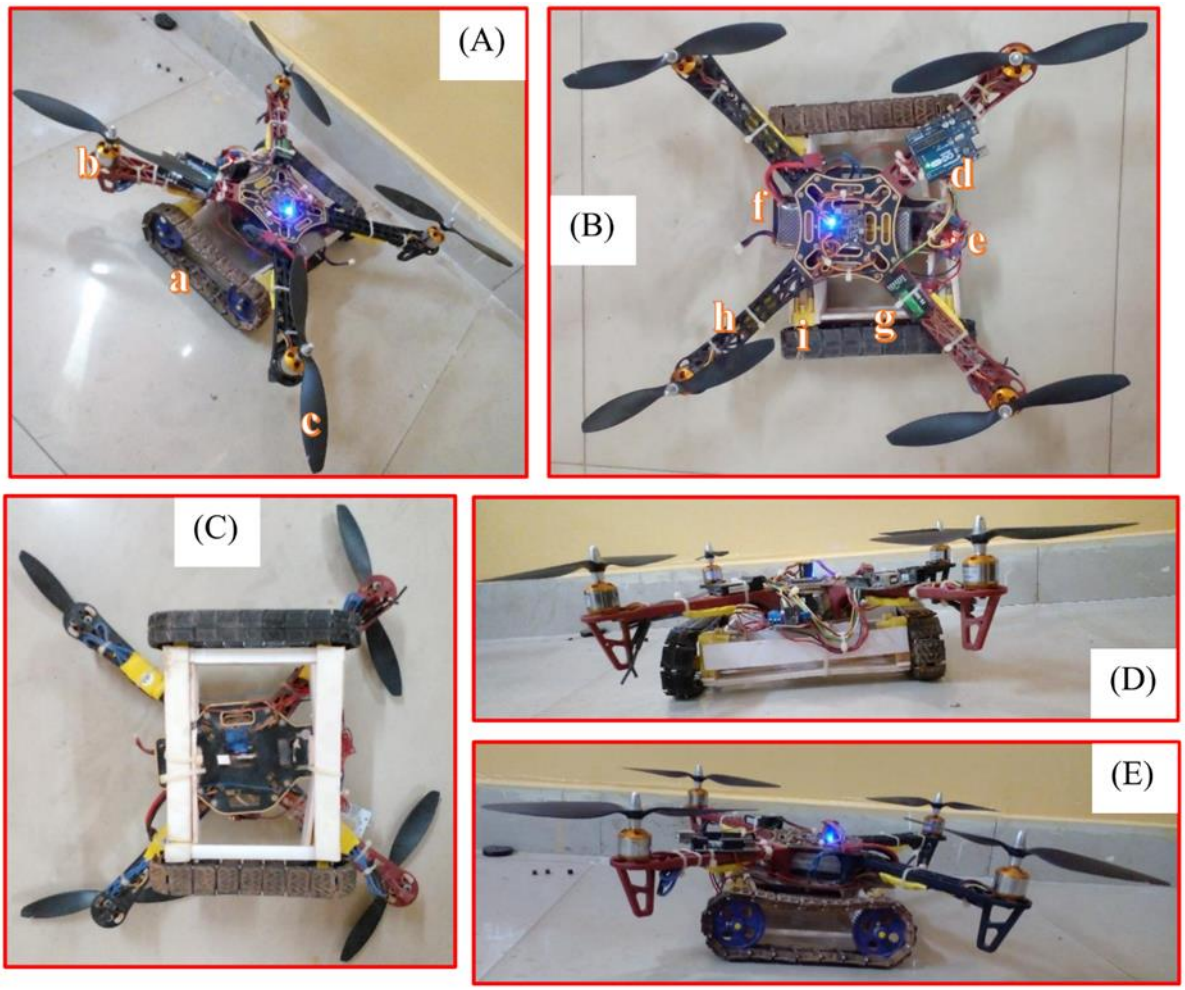

Fig. 9. Snapshots of different views of the physical model of a combined vehicle (UAV + UGV) with the information of various electronic components: (a) Isometric view, (b) Top view, (c) Bottom view, (d) Front view, (e) Side view, (note: a – Caterpillar wheel driving system, b – Brushless motors for rotors, c – Rotors or Blades, d – Arduino microcontroller, e – Motors driver, f – LiPo battery, g – ESC, h – Spider arms, i – DC motors for UGV's wheels. ESC, electronic speed controller; UAV, unmanned aerial vehicle; UGV, unmanned ground vehicle)

Tab. 2. Specifications of various electronic components of a combined vehicle (UAV + UGV)

Name	Specification
Microcontroller	Arduino UNO (ATmega328P)
Switch	On–off switch
Motors for UGV's caterpillar wheel	12 V, 100 RPM, DC Motor
Motors for rotor or blade	Brushless motor, A2212/13T, 1,000 KV
Motors driver for UGV's caterpillar wheel	L298N, dual DC motor driver
Flight controller board	Naze32, Rev6, 32-bit, 6DOF
Transmitter and receiver for a combined vehicle (UAV + UGV)	CT6B Remote six channel transmitter and receiver
ESC	30 Amp
Caterpillar wheels	Wheel radius: 30 mm; Thickness of wheel: 30 mm; Shaft bore diameter: 6 mm
Jumper wire	Male and female jumper wires
Power	Rechargeable lithium–polymer (LiPo) battery, 11.1 V, 3,300 mAh

The UAV's motion is controlled by the remote controller, it provides signals to the UAV's receiver and then the receiver sends the signal to the central flight controller. After that, the flight controller controls the speed of rotors with the help of an ESC. The motion and orientation of the UGV's caterpillar wheel are controlled by four independent DC motors, which provide the required torque during motion on the ground and rough terrain. The differential drive control method is used to control the motion of a vehicle during navigation on the ground. All the DC motors are attached to a combined vehicle's dual DC motor driver. The driver's direction and velocity control pins are connected to the Arduino UNO microcontroller to control the speed and provide left and right turns and backward and forward motions to the vehicle. One lithium–polymer (LiPo) battery of 11.1 V and 3,300 mAh gives power to the vehicle during the ground and aerial motions. The voltage regulator IC-7085 is used to drop from 11.1 V to 5 V and supplies power to the Arduino microcontroller.

Fig. 10. Snapshots of aerial motion control–based experimental results of a combined vehicle (UAV + UGV), (UAV, unmanned aerial vehicle; UGV, unmanned ground vehicle)

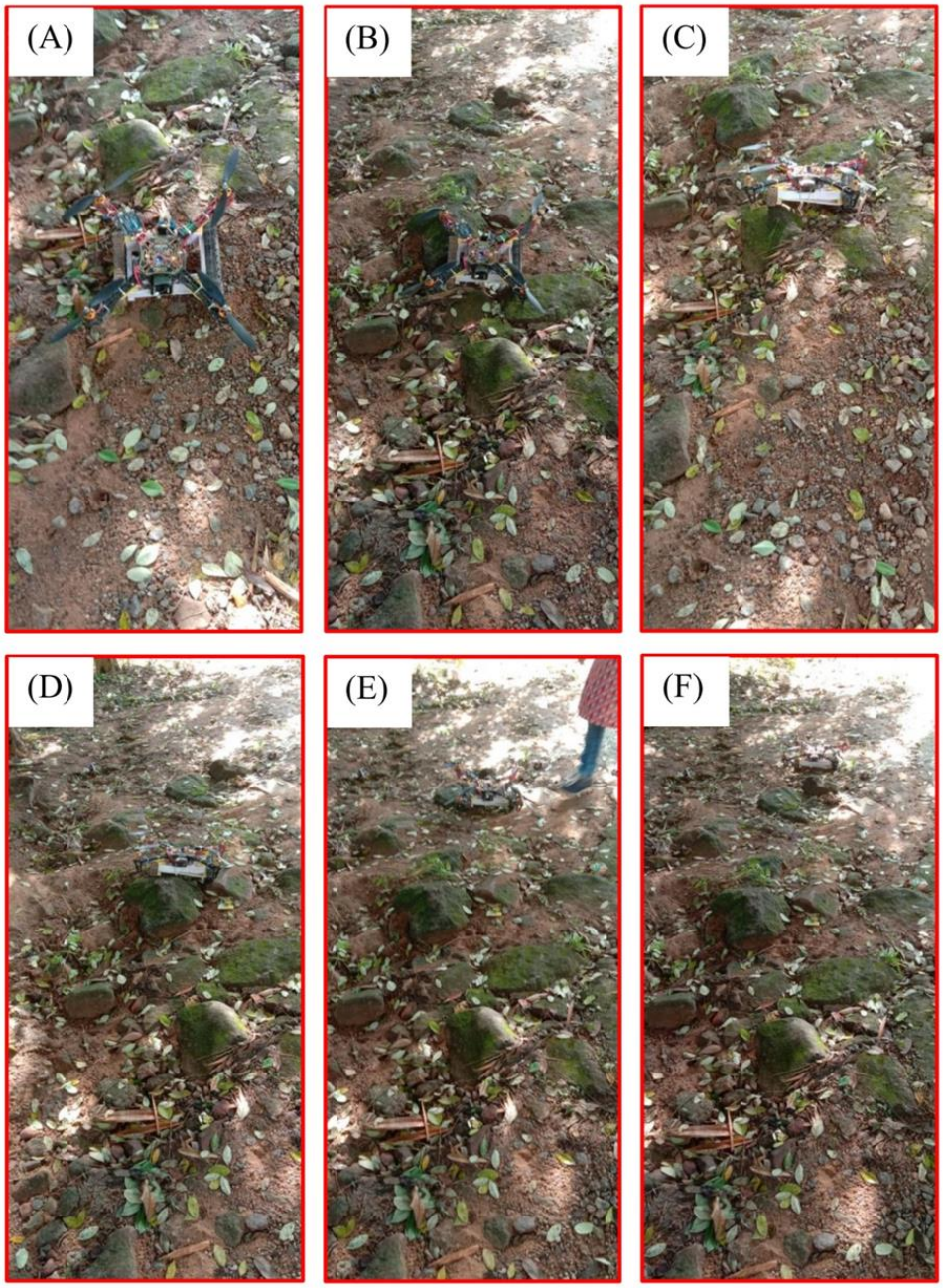

Fig. 11. Navigation result snapshots of a combined vehicle (UAV + UGV) moving on an uneven and rough terrain (UAV, unmanned aerial vehicle; UGV, unmanned ground vehicle)

The various kinematic equations of a combined vehicle (UAV + UGV) mentioned in Section 3 are embedded in the microcontroller to control the flying and ground motions. The kinematic equations of the UAV provide the three translations (linear velocities) and three rotation (angular velocities) commands to the rotors during aerial motion. Similarly, the kinematic equations of the UGV control the velocities and steering of a vehicle during navigation on the ground and rough terrain. We have tested this combined vehicle as an aerial vehicle in the sky and as a ground vehicle on uneven terrain, rough terrain and narrow paths. Fig. 10A–F shows snapshots of aerial motion control–based experimental results of a combined vehicle (UAV + UGV). As shown in the figure, first, the vehicle starts, ready to fly in the sky, and then flies in the sky successfully during our experiment. After conducting the first test of a combined vehicle (UAV + UGV) as an aerial vehicle, we navigate this vehicle on uneven terrain, rough terrain and narrow paths. Fig. 11A–F illustrates the navigation result snapshots of a combined vehicle (UAV + UGV) moving on uneven and rough terrain. In addition, we have run this vehicle in a narrow path to show its robustness, and snapshots of the experimental result are presented in Fig. 12A–E. Moreover, we have also recorded a combined vehicle's real-time linear and angular velocities (UAV + UGV) during both aerial and ground motion tests.

Fig. 13 reveals the real-time recorded linear velocity (meters per second) values of a combined vehicle (UAV + UGV) during the aerial motion control–based experimental results indicated in Fig. 10. Similarly, Figs 14 and 15 show the real-time recorded angular velocity (degrees per second) and linear velocity (meters per second) values of a right- and left-wheel driving system of a combined vehicle (UAV + UGV), respectively, when a vehicle travels on a rough narrow path, as indicated in Fig. 12.

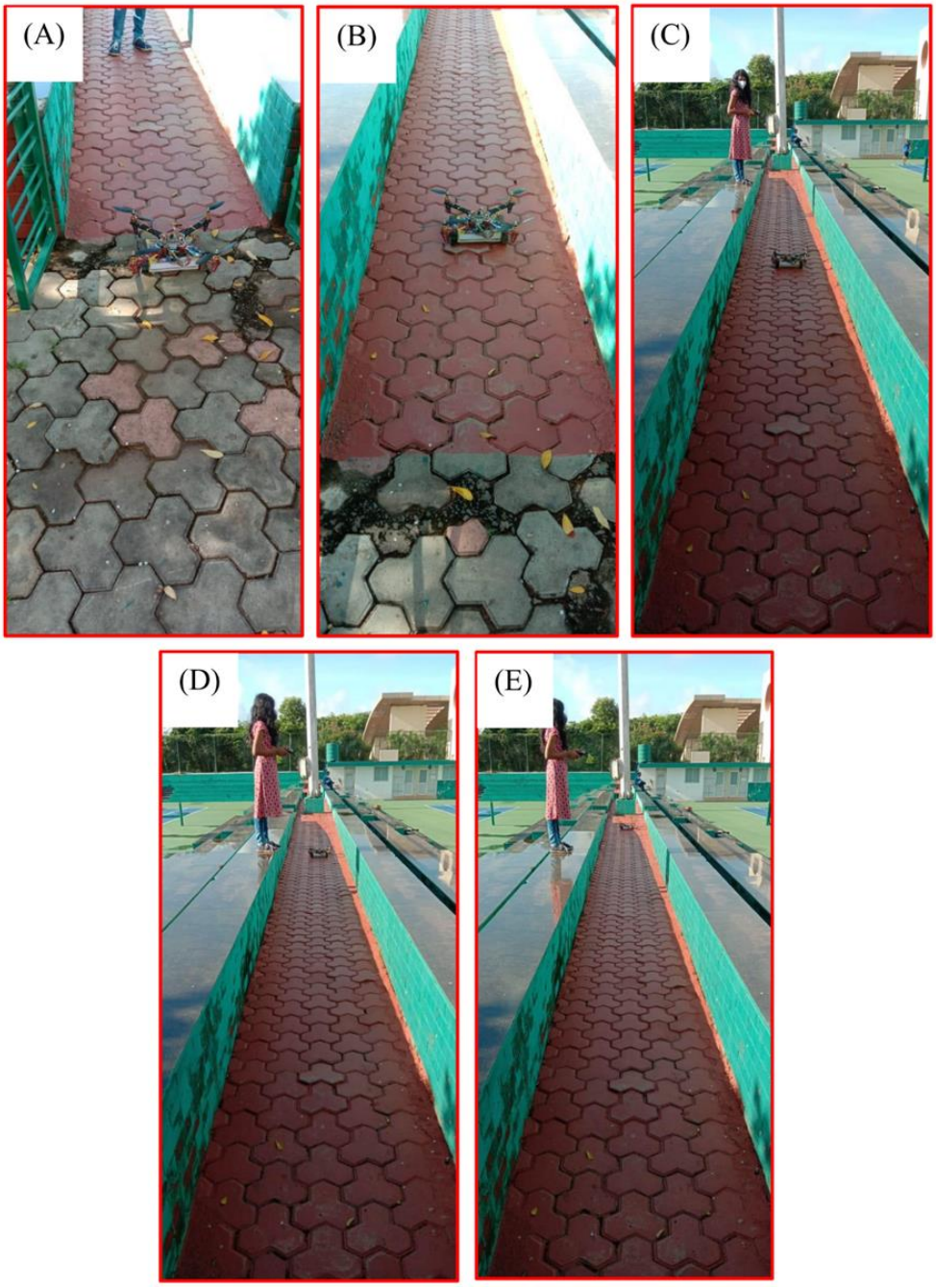

Fig. 12. Snapshots of experimental result of a combined vehicle (UAV + UGV) moving on a rough narrow path, (UAV, unmanned aerial vehicle; UGV, unmanned ground vehicle)

5. CONCLUSION AND FUTURE WORK

In order to provide more flexibility to the existing UAVs or quadcopters, a novel concept-based combined vehicle (UAV + UGV) was designed and studied. The main contribution of this work is the development of a novel concept-based UAV, which can also travel on ground, rough terrain and narrow paths as a UGV according to our requirements. Another objective of this present work was to provide an improved combined vehicle (UAV + UGV) capable of taking off and landing vertically, thereby eliminating the need for any runway. The important contributions of this paper can be summarised as follows: First, the kinematic equations for both a UAV and its attached caterpillar wheel–based UGV are established and implemented in the microcontroller to control the flying and ground motion and orientation of a vehicle (UAV + UGV). Then, using SolidWorks software, the different 2D and 3D pictorial representations of a combined vehicle (UAV + UGV) are displayed. Its various components and their connections with each other are also explained briefly in this investigation. Finally, the presented experimental outcomes confirm that our developed vehicle (UAV + UGV) has given significant results in both air and ground, including rough terrain. Finally, and importantly, our future research work can include dynamic analysis by incorporating Newton–Euler equations to show the reference trajectory tracking control scheme for a combined vehicle (UAV + UGV).

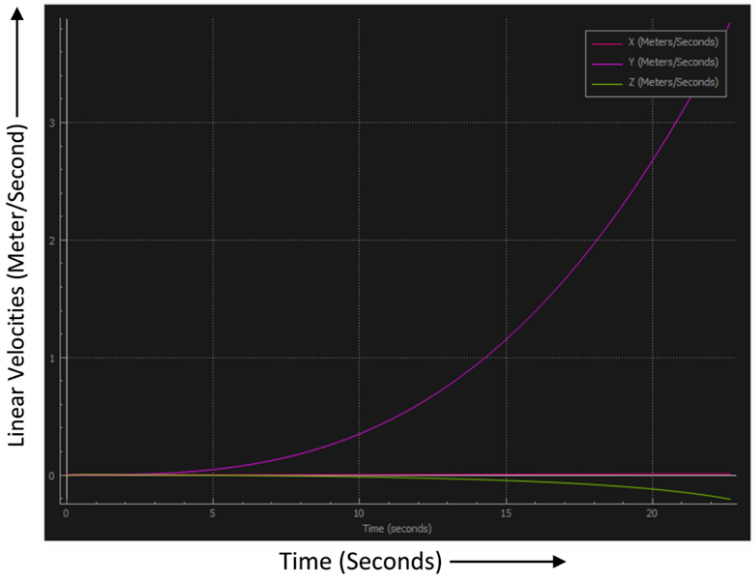

Fig. 13. Real-time recorded linear velocity (meters per second) values of a combined vehicle (UAV + UGV) during the aerial motion control–based experimental results indicated in Fig. 10, (UAV, unmanned aerial vehicle; UGV, unmanned ground vehicle)

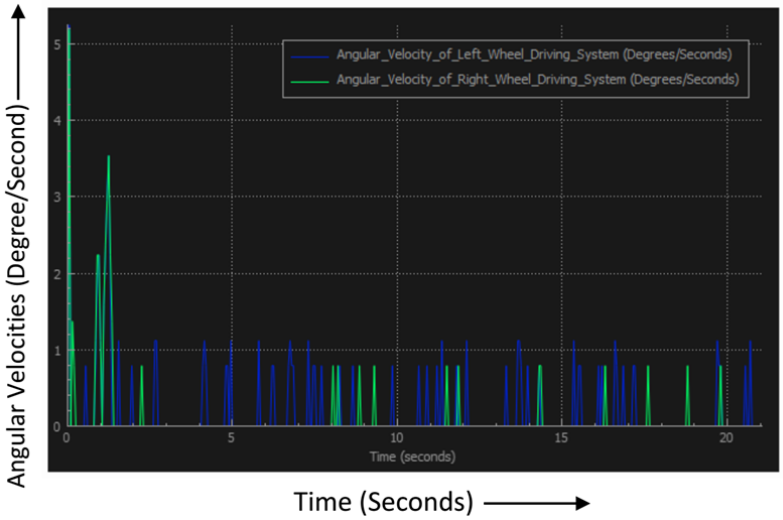

Fig. 14. Real-time recorded angular velocity (degrees per second) values of a right- and left-wheel driving system of a combined vehicle (UAV + UGV), when vehicle travels on a rough narrow path as indicated in Fig. 12, (UAV, unmanned aerial vehicle; UGV, unmanned ground vehicle)

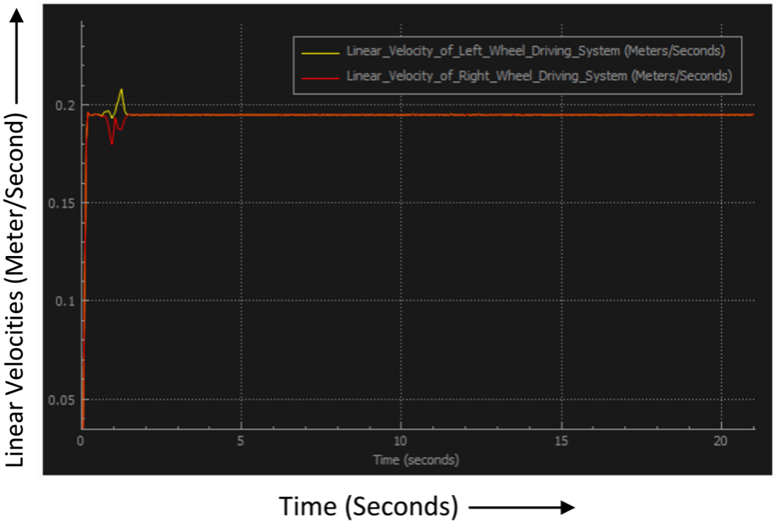

Fig. 15. Real-time recorded linear velocity (meters per second) values of a right- and left-wheel driving system of a combined vehicle (UAV + UGV), when vehicle travels on a rough narrow path as indicated in Fig. 12, (UAV, unmanned aerial vehicle; UGV, unmanned ground vehicle)

REFERENCES

1. Xiang H, Tian L. Development of a low-cost agricultural remote sensing system based on an autonomous unmanned aerial vehicle (UAV). Biosystems Engg. 2011;108(2):174–190.
2. Tahar KN, Ahmad A. A simulation study on the capabilities of rotor wing unmanned aerial vehicle in aerial terrain mapping. Int J of Phy Sci. 2012;7(8):1300–1306.
3. Wang Z, McDonald ST. Convex relaxation for optimal rendezvous of unmanned aerial and ground vehicles, Aero Sci and Tech. 2020;99:1–19.
4. Glida HE, Abdou L, Chelihi A, Sentouh C. Optimal model-free backstepping control for a quadrotor helicopter. Nonlin Dyna. 2020;100(4):3449–3468.
5. Labbadi M, Cherkaoui M. Novel robust super twisting integral sliding mode controller for a quadrotor under external disturbances. Int J of Dyna and Cont. 2020;8:805–815.
6. Hassani H, Mansouri A, Ahaitouf A. Robust autonomous flight for quadrotor UAV based on adaptive nonsingular fast terminal sliding mode control. Int J of Dyna and Cont. 2021;9(2):619–635.
7. Selma B, Chouraqui S, Abouaïssa H. Optimal trajectory tracking control of unmanned aerial vehicle using ANFIS-IPSO system. Int J of Info Techn. 2020;12(2):383–395.
8. Elijah T, Jamisola RS, Tjiparuro Z, Namoshe M (2020). A review on control and maneuvering of cooperative fixed-wing drones. Int J of Dyna and Cont. 202;9(3):1332–1349.
9. Heidari H, Saska M. Trajectory Planning of Quadrotor Systems for Various Objective Functions. Robo. 2021;39(1):137–152.
10. Abdalla M, Al-Baradie S. Real time optimal tuning of quadcopter attitude controller using particle swarm optimization, J of Eng and Techno Sci. 2020;52(5):745–764.
11. Pinto MF, Honório LM, Marcato AL, Dantas MA, Melo AG, Capretz M, Urdiales C. ARCog: An Aerial Robotics Cognitive Architecture. Robo. 2021;39(3):483–502.
12. Xu H, Jiang S, Zhang A. Path Planning for Unmanned Aerial Vehicle Using a Mix-Strategy-Based Gravitational Search Algorithm. IEEE Access, 2021;9:57033–57045.
13. Zhang X, Duan H. An improved constrained differential evolution algorithm for unmanned aerial vehicle global route planning. Appl Soft Comp. 2015;26:270–284.
14. Roberge V, Tarbouchi M, Labonté G. Comparison of parallel genetic algorithm and particle swarm optimization for real-time UAV path planning. IEEE Trans on Indu Informat. 2012;9(1):132–141.
15. Mou C, Qing-Xian W, Chang-Sheng J. A modified ant optimization algorithm for path planning of UCAV. Appl Soft Comp. 2008;8(4):1712–1718.
16. Duan H, Liu S, Wu J. Novel intelligent water drops optimization approach to single UCAV smooth trajectory planning. Aero Sci and Tech, 2009;13(8):442–449.
17. Silva Arantes JD, Silva Arantes MD, Motta Toledo CF, Júnior OT, Williams BC. Heuristic and genetic algorithm approaches for UAV path planning under critical situation. Int J on Art Intel Tools. 2017;26(01):1760008–1760037.
18. Besada-Portas E, De La Torre L, Moreno A, Risco-Martin JL. On the performance comparison of multi-objective evolutionary UAV path planners. Info Sci, 2013;238:111–125.
19. Cui Z, Wang Y. UAV Path Planning Based on Multi-Layer Reinforcement Learning Technique. IEEE Access. 2021;9:59486–59497.
20. Yao M, Zhao M. Unmanned aerial vehicle dynamic path planning in an uncertain environment. Robo. 2015;33(3):611–621.

Ramanuj Kumar: https://orcid.org/0000-0002-4426-2040

Anish Pandey: https://orcid.org/0000-0001-9089-3727

Ashok Kumar Sahoo: https://orcid.org/0000-0003-3785-909X